Short Papers

Design Criteria for Developing an Automated Live-Bird Transfer System

Kok-Meng Lee

Abstract—This paper presents the design criteria for developing machines to automate the process of transferring singulated live birds from a moving conveyor onto a processing line without causing damage or stress. The process includes inserting both legs of the bird into a shackle, then flipping and hanging the bird for subsequent processing. Unlike the traditional articulated robotic arm where the actuations are applied directly through the joint angles, the legs of a live object can only be manipulated indirectly. In addition, natural objects are typically characterized by varying sizes and shapes in batch processing and their natural reflexes (or voluntarily motion) contribute to the overall dynamics. Specifically, this paper illustrates the operating principles of the transfer system and describes the method for manipulating the leg kinematics for shackling. The design criteria have been verified experimentally with live broilers (meat chickens) in a realistic environment. It is expected that the analytical model presented here will provide an essential basis for the design, analysis, and control of the transfer mechanism.

Index Terms—Automation, handling, live bird, mechanical inverter, poultry processing, transfer mechanism.

I. INTRODUCTION

Many industries processing natural products require that live objects be transferred from conveyors to moving processing lines. The repetitive task of transferring live objects is often laborious, unpleasant, and hazardous. In the poultry industry, the task requires individuals to grasp a live broiler by one or both legs and insert both legs into a shackle on a moving conveyor line typically running at speeds of 180 shackles per minute. The birds are usually moved to a dark room to quiet them down in order to facilitate grasping and hanging them. In this dark room, a combination of high-speed conveyors, dust, feathers, pecking, and scratching from the birds creates a hazardous working environment with the potential for a variety of injuries. The unpleasantness of this task sometimes results in high turnover rates at some plants, which requires constant retraining of new employees. In addition, it is extremely difficult to attract new workers to the job. As a result, the live-bird transfer task is an ideal candidate for automation.

Over the past two decades, a number of ideas were proposed to hang live broilers on shackles. Parker [1] developed a method of loading the poultry into a shackle before transporting it from the farm. The same shackle becomes a part of the transport coop structure on which the poultry is restrained during transport. At the processing plant, the shackle with the poultry suspended is loaded directly on the conveyor for further processing. Parker's method has the advantage of reducing the amount of labor required in the overall operation of removing the
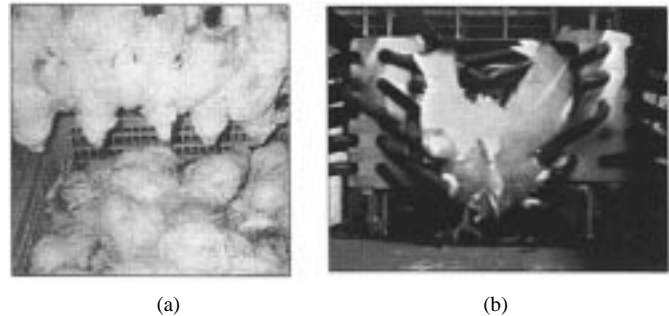
Fig. 1. Comparison of active and nonreactive birds. (a) Bin-picking of nonreactive bird and (b) mechanical grasping of live birds.

poultry from the farm to the processing plant. Several studies [2], [3], however, have suggested that birds held stationary suffered more carcass bruising (particularly bruised drumsticks and broken wings) than they suffer when transported unrestrained. For this reason, developed poultry harvesters are designed to drive birds into module crates that allow multiple birds to move around within the crate and to adjust heat loss by altering posture during transport.

An alternative suggestion was to gas stun/kill the birds before hanging them on the shackle. While it potentially eases manual grasping and hanging processes as the broilers become nonreactive, the attempt to automate nonreactive birds would essentially lead to an unappealing bin-picking process as shown in Fig. 1(a). Bin picking poses no difficulty for human operators, as they are able to visually locate the legs among the overlapping birds and they use a combination of hand–eye coordination and touch to correctly hang the birds on shackles.

Attempts to use vision systems and/or tactile systems that essentially duplicate the human processes have proved more costly and unreliable than desired in high-speed batch processing. A more practical means for rapidly feeding parts to a manufacturing process by a preprogrammed robot has been addressed by a number of researchers as a part-presentation or a part-feeding problem [4]. These methods include the use of vibratory feeders where parts are oriented mechanically and flexible vision-guided part-feeders where machine vision is used to locate the position and orientation of the object on a vibratory feeder [5]–[7]. For polyhedral parts, several researchers (for example, [8], [9]) demonstrated that it is possible to orient parts without the use of a sensor. Flexible part-feeding has found a number of successful industrial automation applications such as machine loading, assembly, and kitting. However, unlike man-made components that are typically rigid and have well-defined shapes and sizes, natural objects such as birds are highly compliant and have no finite polyhedral surface. Irregular shape, loose feathers, and size variation present unique challenges to automated handling. In addition, any unexpected delay between the stunning process prior to manual or automated hanging and the neck cutting/bleeding processes could result in damaging the product.

An important aspect of automating the transfer of a live bird from a conveyor to a shackle is the need to consistently present both legs of a properly oriented bird to the shackle. Heemskerk [10] suggested that spraying water or gas under the abdomen of the bird causes it to stand up, making the bird's legs easier to grasp. Keiter [11] claimed that when birds are rotated on an incline, they naturally orient themselves to face up the slope. Most current studies that are relevant to
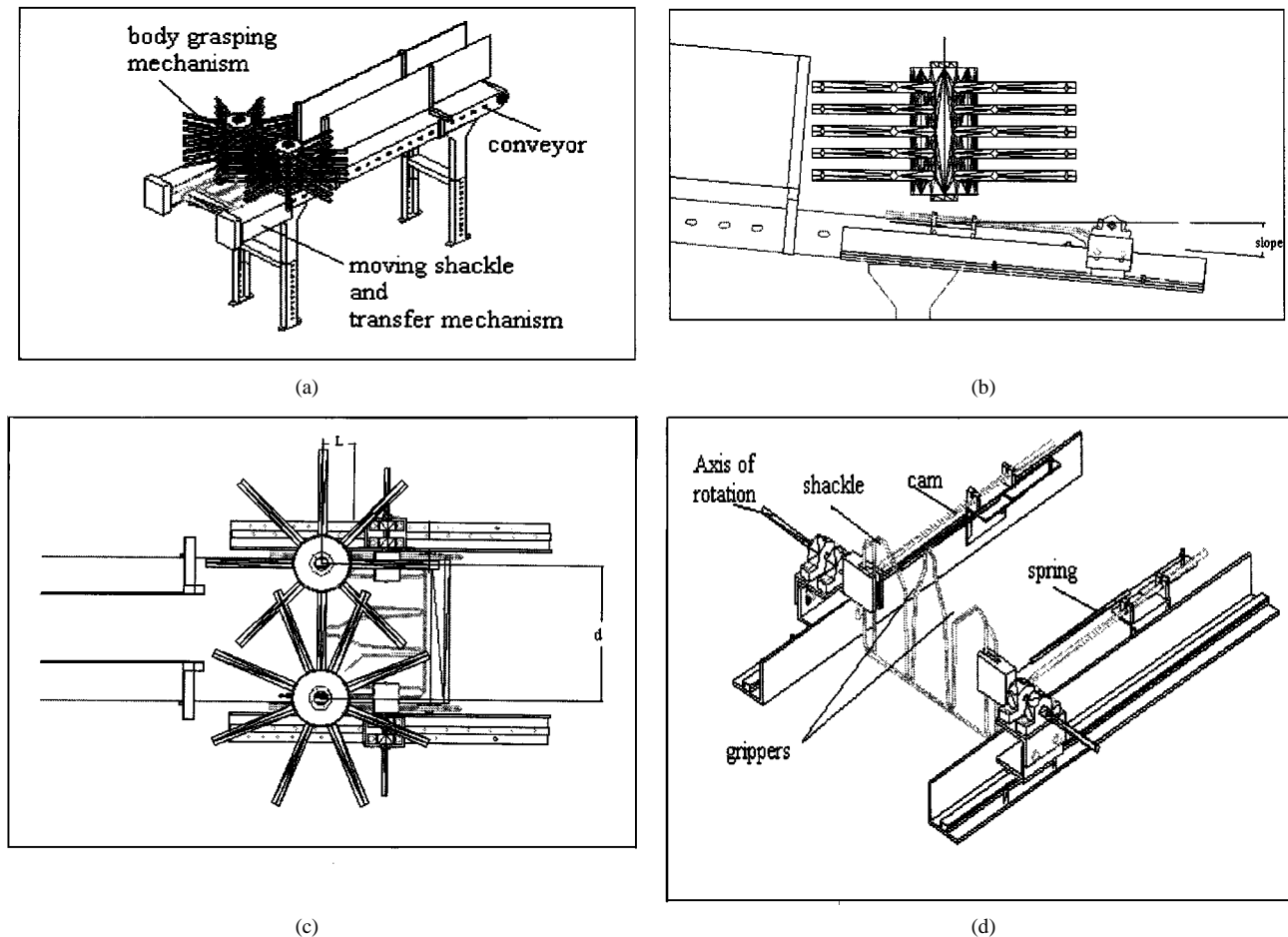
(a)

(b)

(c)

(d)

Fig. 2.   Automated transfer mechanism. (a) CAD model illustrating the design concept. (b) Side view. (c) Plan view. (d) Shackle inverter mechanism.

the live-bird hanging problem have been done on an empirical basis and their results have been assessed subjectively. For these reasons, we have investigated methods of grasping live broilers [12] to facilitate transferring of live birds, leading to the development of a compliant grasper [13]. As compared in Fig. 1, the grasped bird's natural tendency to extend its legs may potentially ease the task of locating the legs. These encouraging results have motivated the author to explore the use of the body-feet velocity difference to manipulate the bird's legs for subsequent processes, which could be electrical or gas stunning. It is worth noting that while most robotic grasping research aims at grasping a static, rigid object in equilibrium, in this investigation the live bird is fed continuously.

Specifically, this paper provides the following.

1)   *It presents the design concept and operational principles of a potentially useful system for transferring live broilers from a moving conveyor to shackles.*

This paper is the first to detail the basic principles of using flexible fingers for manipulating the leg kinematics of a live broiler on a moving conveyor. The system has the ability to accommodate a limited range of varying sizes, shapes, and some motion due to the birds' natural reaction to mechanical grasping.

2)   *It presents a simulation algorithm for assessing the effects of the design changes on the leg kinematics.*

The simulation presented here provides a better understanding of the fundamentals involved in the live-bird transfer system and serves as an essential basis for future design optimization and control of the live-object transfer system. As will be demonstrated in Section IV, the simulation that forms an integral part

of the design process to provide a window for the functioning of the leg-kinematics control process could potentially reduce the number of hardware/software configurations to be tested.

3)   *It presents experimental evaluation of the design with a case study involving live broilers.*

The experiment with live broilers has provided an effective means of verifying the design criteria in a realistic environment. It offers insight into how the birds' natural reflexes contribute to the overall success of the automated transfer of live birds. Along with a discussion of the results, issues to be addressed in the future works are summarized in Section V.

II. DESIGN CONCEPT

Fig. 2 shows the CAD model of a live-bird transfer system that consists of a rotating body-grasper, an inclined conveyor, and a shackle inverter. The grasper is essentially a pair of drums filled with flexible fingers. The two drums, rotating at the same speed but in the opposite direction, move the bird toward the shackle inverter while the fingers constrain the posture of its body. The conveyor is inclined downward with respect to the rotating axes of the drums so that the bird can extend its legs freely between the grasper and the conveyor. Since the bird tends to keep its feet in contact with the conveyor, the legs of the bird can be manipulated by appropriately controlling the drum speed with respect to the conveyor speed.

In operation, the birds are fed in a single file on the inclined conveyor, as shown in Fig. 2(b) and (c), toward the body grasper and the shackle inverter. The shackle is pretensioned to keep it in place until
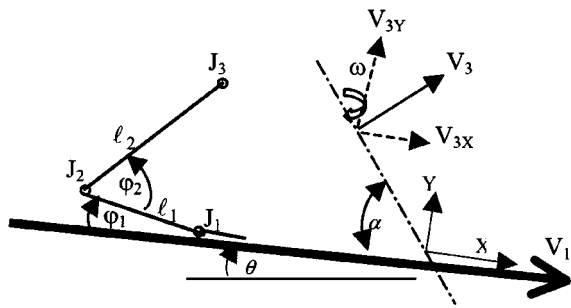
Fig. 3. Leg kinematics on moving conveyor.

the legs are engaged in the grippers. Once the legs are inserted into the grippers, both the bird and the shackle are free to travel together. When the bird/shackle combination reaches the end of the conveyor, the momentum, along with gravity, causes the bird to rotate with the shackle. Fig. 2(d) shows the CAD model of an inverted shackle.

III. OPERATIONAL PRINCIPLES

The success of the automated transfer system depends on: 1) an accurate presentation of the legs to the shackle; 2) the appropriate application of the velocity input to achieve the presentation; and 3) the correct positioning of the shackle for a specified velocity input.

A. Leg-Presentation Kinematics

Fig. 3 illustrates the leg kinematics of a bird, where ℓ_1 and ℓ_2 are the lengths of the lower and upper limbs respectively, J_1, J_2, and J_3 are the toe, hock, and knee joints, respectively, θ is the inclination angle of the conveyor, and α is the angle between the rotating axis and the conveyor. In Fig. 3, the XY coordinate frame is the reference system assigned at the intersection between the rotating axis of the drum and the conveyor. The X and Y axes are directed along and perpendicular to the conveyor surface, respectively. As the feet of the bird are in contact with the conveyor, joint 1 travels on the moving conveyor at a velocity V_1.

The positions of joints 2 and 3 are given as follows:

$$\boldsymbol{J}_{21} = \ell_1 \begin{bmatrix} -\cos\varphi_1 \\ \sin\varphi_1 \end{bmatrix} \tag{1}$$

$$\boldsymbol{J}_{31} = \ell_1 \begin{bmatrix} -\cos\varphi_1 \\ \sin\varphi_1 \end{bmatrix} + \ell_2 \begin{bmatrix} \cos\varphi_{21} \\ \sin\varphi_{21} \end{bmatrix} \tag{2}$$

where $\boldsymbol{J}_{21}$ and $\boldsymbol{J}_{31}$ are the position vectors of joints 2 and 3 with respect to joint 1; $\varphi_{21} = \varphi_2 - \varphi_1 = -\varphi_{12}$ and $\varphi_1 \geq 0$. The bird body, grasped between the finger-filled drums, is translated at a velocity V_3 in the direction perpendicular to the rotating axis. The following equation provides a means to determine the kinematics for presenting the legs to the shackle inverter:

$$\begin{bmatrix} \ell_1 \sin\varphi_1 + \ell_2 \sin\varphi_{21} & -\ell_2 \sin\varphi_{21} \\ \ell_1 \cos\varphi_1 - \ell_2 \cos\varphi_{21} & \ell_2 \cos\varphi_{21} \end{bmatrix} \begin{bmatrix} \dot\varphi_1 \\ \dot\varphi_2 \end{bmatrix}$$
$$= \begin{bmatrix} V_{3X} - V_1 \\ V_{3Y} \end{bmatrix} \tag{3}$$

and the initial conditions are

$$\varphi_1(t=0) = \varphi_{1i}$$
$$\varphi_1(t=0) = \varphi_{2i}$$

where $V_{3X} = V_3 \sin\alpha$ and $V_{3Y} = V_3 \cos\alpha$. Equation (3), a nonlinear differential equation, can be numerically solved for the leg's motion, $\varphi_1(t)$ and $\varphi_2(t)$, the solution of which depends on the size of the bird, the drum speed, and initial conditions. Although the conveyor inclination θ does not directly appear in (3), it will be shown in Section IV
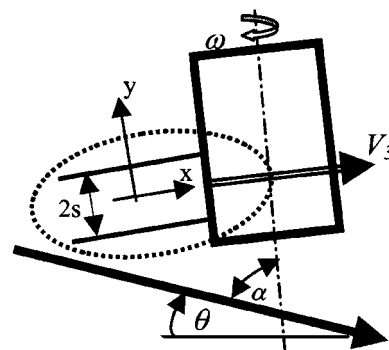
(a)
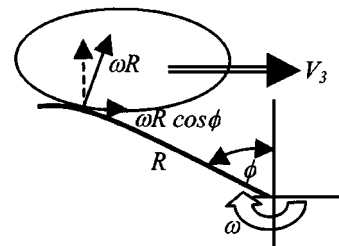
(b)

Fig. 4. Drum speed determination. (a) Side view and (b) plan view in the direction of the axis.

that the conveyor inclination has a significant influence on the initial condition since birds react on moving inclined surfaces.

B. Application of the Velocity Input-Drum Speed

The method for predicting the contact force exerted by a rotating finger on the bird can be found in [12], [14]. The finger exerts a force $\boldsymbol{f}$ at the contact point as the drums rotate. For a positive grasp, $\mu\boldsymbol{f}_n > \boldsymbol{f}_t$ such that the finger would not slip past the object, where

μ static coefficient of friction between the bird and the finger;
f_n normal component of the contact force;
f_t tangential component of the contact force.

To determine the drum speed for a specified body velocity, we model the body of the broiler as an ellipsoid

$$\frac{x^2}{\eta^2} + \frac{y^2}{\lambda^2} + \frac{z^2}{\gamma^2} = 1 \tag{4}$$

where η, λ, and γ are characteristic radii of the ellipsoid. As the finger rotates, it intercepts the ellipsoid at $y = y_i$ ($|y_i| < \lambda$). The cross section intercepted by the rotating finger is essentially an ellipse

$$\frac{x^2}{a_s^2} + \frac{z^2}{b_s^2} = 1 \tag{5}$$

where $a_s^2 = \eta^2[1 - (y_i^2/\lambda^2)]$ and $b_s^2 = \gamma^2[1 - (y_i^2/\lambda^2)]$. For a positive, symmetric grasping (with no slip at the contact surface), the bird and the finger have the same velocity at the contact point and thus the bird translates along the centerline between the two drums as shown in Fig. 4, where 2s is the spacing between the two adjacent rows of fingers.

Since the broiler and the finger have the same velocity at the contact point, the magnitude of the velocity at joint 3 is

$$|\boldsymbol{V}_3| = |\omega R \cos\phi| \tag{6}$$

where

ω angular speed of the drum;
R distance of the contact point from the axis;
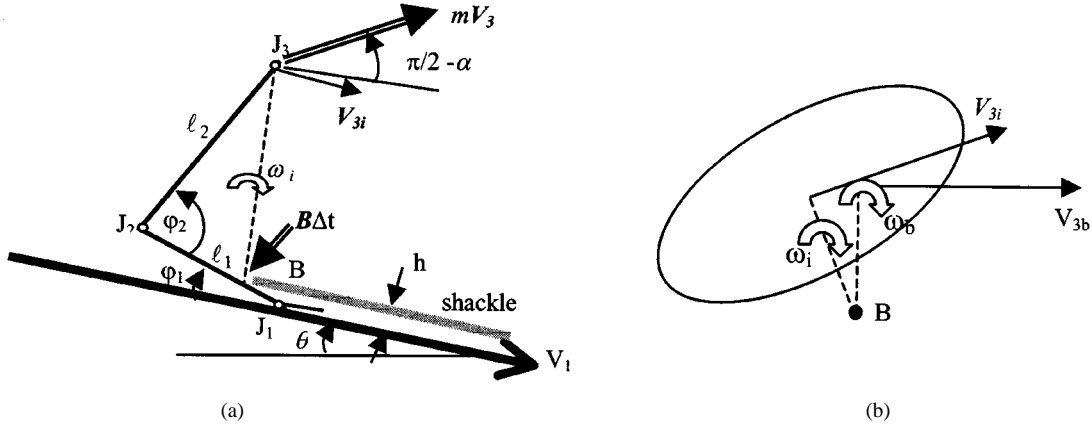ϕ angle is defined as shown in the plan view of Fig. 4.

Fig. 5.   Kinematics at the point of impact.

For a small variation of $\omega R \cos \phi$, the drum speed can be approximated by

$$\omega = \frac{2}{d - 2b_s} |V_3| \qquad (7)$$

where ω is the angular speed of the drum, d is the distance between the rotational axes of the two drums, and $(d - 2b_s)/2 > 0$ since it is greater than the radius of the rotating drum.

C. Shackle Location and Limiting Input Velocity

When one or both of its legs strike the shackle at point B, the impact could cause the bird to rotate about B, as shown in Fig. 5. The stability depends on the shackle position as well as the location of the center of gravity (CG) relative to its feet during the impact. If the CG is ahead of the critical position at which it is directly above point B during the impact, the momentum together with the gravity could cause the bird to trip over.

In order to prevent the bird from toppling over before the legs are gripped, it is desired to derive an expression for the limiting value of V_3. We make the following assumptions in the subsequent derivation: 1) based on observation of a bird's posture in equilibrium, the bird's CG is approximated at the mid-point between its knee joints; 2) the impact at B is assumed to be perfectly plastic; 3) the mass of the paw is negligible; and 4) the only impulsive force external to the bird is the impulse reaction at B. The position vector of the point B with respect to joint 1 is

$$\boldsymbol{J}_{B1} = \begin{bmatrix} -h \cot \varphi_1 \\ h \end{bmatrix} \qquad (8)$$

where h is the spacing between the shackle and the conveyor.

$$\boldsymbol{J}_{3B} = \boldsymbol{J}_{31} - \boldsymbol{J}_{B1}. \qquad (9)$$

We apply the principle of impulse and momentum to the bird about B. Together with the bird's rotational inertia $I_z = (1/5)m(\eta^2 + \lambda^2)$ where m is the mass of the bird, we have

$$V_3 = \frac{J_{3B}^2 + \frac{1}{5}\left(\eta^2 + \lambda^2\right)}{Y_{3B} \sin \alpha + X_{3B} \cos \alpha} \omega_i \qquad (10)$$

where $J_{3B} = |\boldsymbol{J}_{3B}|$ and X_{3B} and Y_{3B} are the X- and Y-components of $\boldsymbol{J}_{3B}$, respectively. Using the law of cosine, we have

$$J_{3B}^2 = \left(\ell_1 - \frac{h}{\sin \varphi_1}\right)^2 + \ell_2^2 - 2\left(\ell_1 - \frac{h}{\sin \varphi_1}\right)\ell_2 \cos \varphi_2. \quad (11)$$
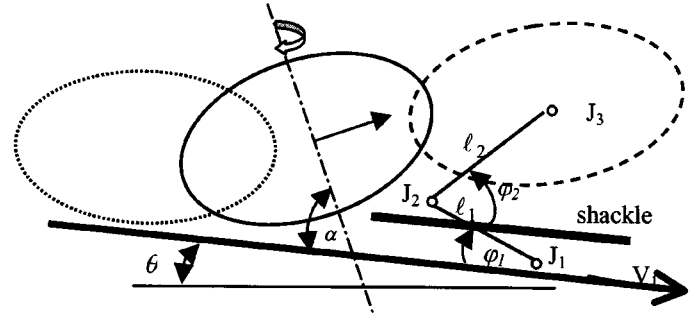

Fig. 6.   Trajectory specification and motion constraints.

TABLE I
SIMULATION PARAMETERS

Location of grippers' entry	L=150mm (6 in.), h=25mm (1 in.)
Finger spacing:	2s = 50mm (2 in)
Drum radius:	81.25mm (3.25 in)
Spacing between axes:	d= 362.5mm (14.5 in.)
Conveyor parameters:	α=82.5°; θ=7.5°; V_1=0.375 m/s (15 in/s)
Average bird size:	2η=195mm; 2λ=112mm; 2γ=132mm
Average lengths of the leg:	ℓ_1=72mm (2.9 in); ℓ_2=95mm (3.8 in)
Typical "sit-down" posture:	φ_{1i}=0°; φ_{2i}=45°

The body should not have any kinetic energy when the CG is directly above B in order to prevent the bird from toppling over. Thus, we choose $V_{3b} = 0 (\Rightarrow \omega_b = 0)$ and apply the principle of conservation of energy between the initial and the critical positions, which yields

$$T_i = mg J_{3B} \left(1 - \cos \beta\right) \qquad (12)$$

where the kinetic energy at the instant of impact is given by

$$T_i = \frac{1}{2}mV_{3i}^2 + \frac{1}{2}I_z \omega_i^2 = \frac{m}{2}\left[J_{3B}^2 + \frac{1}{5}(\eta^2 + \lambda^2)\right]\omega_i^2 \qquad (13)$$

where $\beta = \tan^{-1}\left(|X_{3B}|/|Y_{3B}|\right) - \theta$ and $X_{3B} \leq 0$. Substituting (13) into (12) yields

$$\omega_i^2 = 2g \frac{J_{3B}\left[1 - \cos \beta\right]}{J_{3B}^2 + \frac{1}{5}(\eta^2 + \lambda^2)}. \qquad (14)$$

Thus, the limiting magnitude for the velocity V_3 is given by

$$V_3 \leq \frac{\sqrt{2g J_{3B}\left(1 - \cos \beta\right)\left(J_{3B}^2 + \frac{1}{5}(\eta^2 + \lambda^2)\right)}}{Y_{3B}\sin \alpha + X_{3B}\cos \alpha} \qquad (15)$$
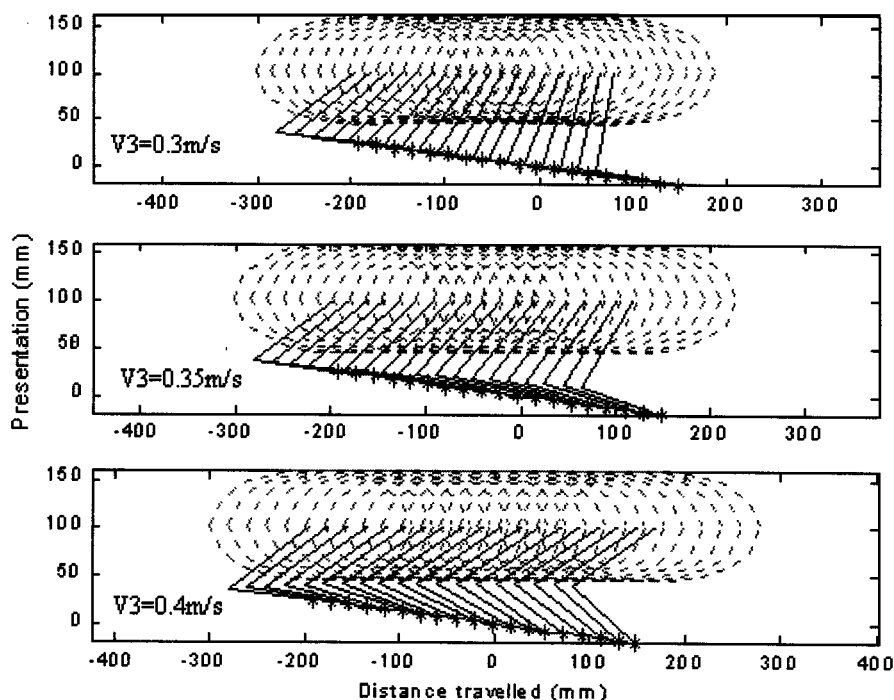
Fig. 7. Tradeoff between pressure on hock joint and stability.

which is a function of the leg presentation at the instant of impact. For constant V_1 and V_3, this presentation (or the joint angles) can be expressed in terms of input velocity difference as

$$\varphi_2 = \cos^{-1} \frac{\ell_1^2 + \ell_2^2 - (X_{31}^2 + Y_{31}^2)}{2\ell_1 \ell_2} \tag{16}$$

$$\varphi_1 = \tan^{-1} \frac{Y_{31}}{X_{31}} - \tan^{-1} \frac{\ell_2 \sin \varphi_2}{\ell_1 - \ell_2 \cos \varphi_2} \tag{17}$$

and

$$\begin{bmatrix} X_{31} \\ Y_{31} \end{bmatrix} = \boldsymbol{J}_{31i} + \begin{bmatrix} (V_{3X} - V_1)(t - t_i) \\ V_{3Y}(t - t_i) \end{bmatrix} \tag{18}$$

where $\boldsymbol{J}_{31i}$ is the initial leg posture before entering the grasper.

IV. DESIGN CRITERIA AND EVALUATION

In order to provide a quantitative measure for evaluating the performance of a live-bird transfer system design in a realistic processing facility, we define the following measures:

- *Average Hanging-Performance-Index ($\overline{\mathrm{HPI}}$):*
  The HPI value, which ranges from 0 to 5, is a measure of how well the bird is hung:
  HPI = **0**– when the bird is hung by two legs;
  HPI = **1**– when the bird is hung by one leg and one hock;
  HPI = **2**– when the bird is hung by two hocks;
  HPI = **3**– when the bird is hung by only one leg;
  HPI = **4**– when the bird is hung by only one hock;
  HPI = **5**– if the bird escapes hanging.
- *% Success (%S)*= % of birds hung with $\mathrm{HPI} < 3$.
- *% Failure (%F)*= % of birds escape handing (or $\mathrm{HPI} = 5$).

Since a detailed discussion of the compliant grasping mechanism design can be found in [12] and [13], this study focuses on the following design parameters that could potentially affect the system performance: 1) the conveyor inclination; 2) the angle between the axis and the conveyor surface; 3) the location of the shackle with respect to the drum axes; and 4) the operating drum speed with respect to that of the con-

TABLE II
BIRD CHARACTERISTICS

	Female (57 birds)		Male (63 birds)	
	Mean	Std. dev.	Mean	Std. dev.
Weight (kg)	1.56	0.12	1.76	0.18
Body height, mm (in)	110 (4.4)	10 (0.4)	115 (4.6)	12.5 (0.5)
Body length/height	1.7	0.1	1.7	0.2
Body width/height	1.2	0.1	1.2	0.1

veyor. These parameters must be designed along with considerations of the bird's visual responses to mechanical grasping and manipulation.

A. Entry Posture

It is desired to keep the variation in the birds' initial postures and natural reflexes to mechanical processes as uniform as possible in order to minimize the demand on the control efforts of the transfer system. Based on the following observations, we choose "sitting" as a preferred entry posture.

1) As food is usually withheld for 8–12 h, water 1 h before catching to reduce risk of carcass contamination at the processing plant; most of the birds are typically weary.
2) Birds tend to sit when they are in darkness.
3) In order to avoid the fingers from swiping the legs, it is desired to have the bird sit as it enters.

Preliminary experiments using live birds have suggested that birds dislike (and become panicked on) slippery surfaces. With an inclined plane where the coefficient of friction between the surface and a sitting bird was estimated experimentally to be $\mu = \tan 25° = 0.4768$, the bird's tendency was to sit when the surface is moderately inclined (15° or less), apparently to lower its CG for stability. When the downward-inclined plane was moving, the bird was observed to lean back (sit up) in order to maintain its balance. Too large an inclination angle or a conveyor speed caused the bird to become nervous.

When the bird sits, $\varphi_1 = 0$ and thus the derivative should be positive or $\dot{\varphi}_1 \geq 0$. Otherwise, the bird will be forced to lean back involuntarily.

(a)   (b)

Fig. 8.   Experimental test-bed. (a) Side view and (b) front view.

(a)   (b)
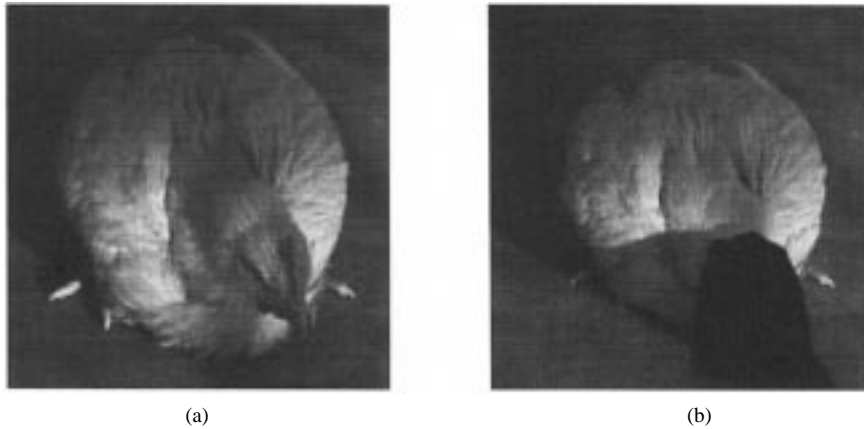
Fig. 9.   Bird with and without vision (in sitting posture). (a) Bird with vision. (b) Bird in complete darkness, covered by a hood.

TABLE III
ENTRY POSTURES ($V_1 = 0.375$ m/s OR 15 IN/S)

	With Vision			Without Vision		
	$\theta=0°$	$\theta=7.5°$	$\theta=15°$	$\theta=0°$	$\theta=7.5°$	$\theta=15°$
sit down	35%	25%	5%	80%	100%	85%
sit up	45%	50%	75%	10%	0%	10%
stand	20%	25%	20%	10%	0%	5%

TABLE IV
EFFECTS OF BIRD SIZE ($\omega = 21.5$ rpm, $\alpha = 75°$)

Bird Size	Minimum	Average	Maximum
V_3 m/s (in/s)	0.353 (14.13)	0.341 (13.62)	0.322 (13.04)
b_s mm (inch)	49 (1.95)	68 (2.37)	76 (3.03)
X_{3B} mm (inch)	−1.25 (−0.05)	−16.5 (−0.66)	−34 (−1.36)
Y_{21} mm (inch)	25 (0.99)	19 (0.761)	10.9 (0.44)

This involuntarily motion, which causes the hocks (or joint 2) and the tail to press against the conveyor surface, could strain the limbs and have a potential to damage product quality. The condition for the velocity input such that $\dot{\varphi}_1 \geq 0$ can be derived by eliminating $\dot{\varphi}_2$ from (3), which is accomplished by multiplying the first and second rows of (3) by $\cos \varphi_{12}$ and $\sin \varphi_{12}$, respectively, and then summing the resulting equations. Upon simplifying, we have

$$(\ell_1 \sin \varphi_2) \dot{\varphi}_1 = V_3 \sin(\alpha + \varphi_{21}) - V_1 \cos \varphi_{21}. \qquad (19)$$

Thus, the condition $\dot{\varphi}_1 \geq 0$ implies

$$V_3 \geq \frac{\cos \varphi_{21}}{\sin(\alpha + \varphi_{21})} V_1 \qquad (20)$$

where $0 < \alpha < (\pi/2)$ and $\varphi_2 > 0$. Note that, when $\varphi_1 = 0$, $\varphi_{21} = \varphi_2$. Equation (20) imposes the lower limit of the velocity input when the bird enters with a sitting posture.

B. Design Parameters and Operating Speed

For a specified conveyor inclination and speed, the velocity of the bird body must satisfy the following constraints imposed by the location of the shackle as shown in Fig. 6:

1) the bird's body must be lifted over the shackle;
2) the shackle must grip the lower limbs of the bird.

The parameters that could be designed to satisfy the constraints include the angle between the conveyor and the drum axes, the rotating speed of the grasper, and the location of the shackle. To reduce the combination of hardware/software configurations to be tested, a simulation algorithm has been written based on the equations detailed in Section III. The effects of the design changes on the leg kinematics were studied using simulation. The values of the design parameters estimated are summarized in Table I.

For a given conveyor speed of 0.375 m/s, the lowest acceptable body speed can be calculated from (20) to be 0.3396 m/s (13.37 in/s). As

TABLE V
PERFORMANCE COMPARISIONS ($\overline{HPI}, \%S, \%F$)

| | Vision | | Without Vision (hooded bird) | |
	$\alpha=75°$	$\alpha=90°$	$\alpha=75°$	$\alpha=90°$
$\theta=0°$	4.1, 10, 50	4.2, 10, 70	4.6, 60, 10	3.9, 10, 40
$\theta=7.5°$	3.3, 40, 30	3.0, 40, 10	1.0, 100, 0	2.4, 60, 20
$\theta=15°$	3.8, 20, 50	2.2, 80, 10	2.9, 40, 20	2.5, 60, 10

illustrated in Fig. 7, a relatively low body-to-feet velocity will result in two problems: 1) significant pressure on the hock joint and 2) the insufficient lift of the hock joint. On the other hand, too high a body-speed will cause the bird to topple over the shackle before the legs are gripped.

C. Experimental Verification with Live Birds

Fig. 8 shows the experimental test-bed used in evaluating the transferring system design, where θ and α can be independently adjusted. Specific values of the parameters were determined using a hybrid design technique of computer simulation and experimentation involving live broilers. Twelve different experimental trials were conducted with 120 novice broilers (57 female and 63 male) from a poultry processing plant to examine the key parameters that significantly affect the birds' entry-posture and to evaluate the system performance. These broilers' characteristic dimensions are summarized in Table II.

The experimental trials involved three conveyor angles ($\theta = 0, 7.5°$ and $15°$) and two shaft-conveyor angles ($\alpha = 75°$ and $90°$), and in each pair of angles the entry postures with and without bird's vision (Fig. 9) were experimentally compared. For each of the 12 trials, 10 birds were used. The bird was placed on a 6-ft (1.8-m) conveyor moving at 0.375 m/s (or 15 in/s). Its presentations before entering the grasper at 1.2 m (or 48 in) from the point of drop-off and after inverting the shackle were imaged for analysis.

Entry Posture: The observed postures are compared in Table III, where each conveyor-inclination trial includes 20 birds regardless of the α values. The results show that the bird's visual reflex has a significant effect on its posture before entering the grasper. Of the 60 birds tested without vision, over 80% of the birds were found to sit still as they entered the grasper and the preferred conveyor inclination was found to be $\theta = 7.5°$ at which all 20 birds maintained a sitting posture as shown in Fig. 9(b).

Numerical Simulation: The effects of the size variation on the relative location of the CG and the lift of the hock joint were studied numerically for the range of birds characterized by $(175, 100, 112)_{\min}$, $(195, 123, 133)_{\text{mean}}$, and $(212, 137, 162)_{\max}$ where $(2\eta, 2\lambda, 2\gamma)$ are in mm. The tradeoffs have led to a preferred nominal drum speed of 21.5 rpm at $\alpha = 75°$. The results are summarized in Table IV.

Experimental Evaluation: The results are compared in Table V, each of which involved 10 hooded birds (without vision) and the drum speed, measured experimentally, was 21.5 ± 1.5 rpm. The two α values are $75°$, a preferred value among simulation tradeoffs and $90°$ at which the drum axes are perpendicular to the conveyor and thus the lift is only provided by the speed difference $V_3 - V_1$. Table V compares the results of the six trials. As expected, the entry posture and the two inclination angles have significant effects on the performance of the transfer system. The best performance has been the trial with $\theta = 7.5°$ and $\alpha = 75°$, which has a 100% success of hanging all the 10 hooded birds entering with a "sit-down" posture. The corresponding HPI distribution was ($HPI = 0 : 3, HPI = 1 : 4$ and $HPI = 2 : 3$).

V. CONCLUSION

The design concept of an automated live-bird transfer system has been developed. The system uses the body-to-feet velocity difference to manipulate the leg kinematics of the bird, thereby provides an effective means to insert both legs of the bird to a shackle. The system has the ability to accommodate a limited range of varying sizes, shapes, and some motion due to the birds' natural reaction to mechanical grasping.

The operational principles, which provide a better understanding of the processes involved in the transfer system and a basis for the development of the simulation algorithm, have been presented. Simulation has been shown to be an effective tool to describe the tradeoff between the bird stability and the hock location for a limited range of size and shape variations. It is expected that the analysis presented here will provide an essential basis for the design optimization, analysis and control of the transfer mechanism.

Using a hybrid design technique (a combination of motion simulation and experimentation), key parameters that have significant influence on the success rate of hanging live broilers have been identified and verified experimentally with live birds. The results show that the birds' visual response to the mechanical grasper and the conveyor inclination for a specified speed and coefficient of friction have significant effects on its entry posture.

Current efforts are directed toward evaluating the bird's visual acuity in different spectral environments, using a posture-dependent drum speed profile to improve the hanging performance and developing predictive models to analyze the effect of contact forces on tissue damage and carcass quality.

REFERENCES

[1] A. E. Parker Jr, "Method and Apparatus for Handling Live Poultry," U.S. Patent 3 796 192, 1974.

[2] P. J. Kettlewell and M. J. Turner, "A review of broiler chicken catching and transport systems," *J. Agricultur. Eng. Res.*, vol. 31, pp. 93–114, 1985.

[3] G. B. Scott, "Poultry handling: A review of mechanical devices and their effect on broiler welfare," *World's Poultry Sci. J.*, vol. 49, pp. 44–57, Mar. 1993.

[4] K-M. Lee, "Flexible part-feeding system for machine loading and assembly. Part I: A state-of-the-art survey. Part-II: A cost-effective solution," *Int. J. Production Econom.*, vol. 25, pp. 141–168, 1991.

[5] B. Carlisle, K. Goldberg, A. Rao, and J. Wiegley, "A pivoting gripper for feeding industrial parts," in *IEEE Int. Conf. Robot. Automat.*, San Diego, CA, May 1994, pp. 1650–1655.

[6] K-M. Lee, "Design concept of an integrated vision system for cost-effective flexible part-feeding applications," *ASME Trans. J. Eng. Industry*, vol. 116, pp. 421–428, Nov. 1994.

[7] K-M. Lee and Y.-F. Qian, "Development of a flexible intelligent control for target pursuit," *ASME Trans. J. Manufact. Sci. Eng.*, vol. 120, pp. 640–647, Aug. 1998.

[8] M. A. Erdmann and M. T. Mason, "An exploration of sensorless manipulation," *IEEE J. Robot. Automat.*, vol. 4, pp. 369–379, Aug. 1988.

[9] A. Rao, D. J. Kriegman, and K. Goldberg, "Complete algorithms for feeding polyhedral parts using pivot grasp," *IEEE Trans. Robot. Automat.*, vol. 12, pp. 331–342, Apr. 1996.

[10] W. J. C. Heemskerk, "Method for Causing Sitting Poultry to Stand up and Apparatus for Carrying out this Method," U.S. Patent 5 088 959, 1992.

[11] M. E. Keiter, "Method and Apparatus for Orienting Live Poultry," U.S. Patent 5 129 857, 1992.

[12] K-M. Lee, "On the development of a compliant grasping mechanism for on-line handling of live objects, Part I: Analytical model," in *IEEE/ASME Int. Conf. Adv. Intell. Mechatron. (AIM'99)*, Atlanta, GA, Sept. 19–23, 1999, pp. 354–359.

[13] K-M. Lee, B. Webster, J. Joni, X. Yin, R. Carey, M. Lacy, and R. Gogate, "On the development of a compliant grasping mechanism for on-line handling of live objects, part II: Design and experimental investigation," in *AIM'99*, Atlanta, GA, Sept. 19–23, 1999, pp. 360–365.

[14] K-M. Lee, J. Joni, and X. Yin, "Compliant grasping force modeling for handling of live objects," in *Proc. 2001 IEEE ICRA*, Seoul, Korea, May 21–26, 2001, pp. 1059–1064.

Autonomous Vehicle Navigation Utilizing Electrostatic Potential Fields and Fuzzy Logic

Nikos C. Tsourveloudis, Kimon P. Valavanis, and Timothy Hebert

Abstract—An electrostatic potential field (EPF) path planner is combined with a two-layered fuzzy logic inference engine and implemented for real-time mobile robot navigation in a 2-D dynamic environment. The environment is first mapped into a resistor network; an electrostatic potential field is then created through current injection into the network. The path of maximum current through the network corresponds to the approximately optimum path in the environment. The first layer of the fuzzy logic inference engine performs sensor fusion from sensor readings into a fuzzy variable, *collision*, providing information about possible collisions in four directions, *front*, *back*, *left*, and *right*. The second layer guarantees collision avoidance with dynamic obstacles while following the trajectory generated by the electrostatic potential field. The proposed approach is experimentally tested using the *Nomad 200* mobile robot.

Index Terms—Collision avoidance, dynamic environment, fuzzy logic, mobile robots, navigation, path planning, potential fields, sensor fusion.

I. INTRODUCTION

This paper is the natural outgrowth of recently published research [44]. It presents a novel approach to solving the autonomous mobile robot (AMR) navigation problem in 2-D dynamic environments, by combining the electrostatic potential field (EPF) path planner (already presented in [44]) with a two-layered fuzzy logic (FL) inference

engine, operating in tandem to plan, replan, and execute a collision free path in real-time. Tasks are performed by the object detection, localization, path planning, and collision avoidance modules, including on-line sonar sensor-based environment map generation and trajectory following [17].

The main idea and contribution for the proposed EPF/FL planner is to combine "planned and reactive behavior." Given a 2-D environment (with initial information from potentially existing environment *a priori* maps and on-line sonar sensor data), the EPF plans the initial trajectory and starts executing it via the motion control module (see Fig. 1). Once the object detection module (working in parallel with the EPF) detects through sensor readings a "high collision possibility," it forces the motion control module to "forget" the initial EPF path, take corrective actions in terms of robot steering and robot speed to avoid the collision, until new sensor readings dictate a "low" or "not-possible" collision possibility (FL-reactive). Then, the motion control module takes into account the initial trajectory as computed at this time instant by the EPF planner. The EPF planner is reinvoked every time the environment map is updated. An additional contribution of the proposed approach is that it considers a complete sensor-based model of the robot environment and makes no assumption regarding the location or trajectory of the obstacles. In further detail, the EPF/FL planner works as follows.

Using approximate cell decomposition, the environment is first mapped onto a resistor network allowing a current source and a current sink to be placed at the initial and goal positions, respectively. Each (square) cell is actually represented by a node with eight resistors connected to the neighboring cells, unless the cell is located in the boundary of the map in which case those resistors on the outer edges are left open circuited. The current flow through the network establishes a true potential field, whose negative gradient may be followed in a "quickest descent" method to generate in real-time, (approximately) optimal local minima free trajectories (static environments), which may be modified at each sampling instant to account for dynamic obstacles. Thus, a completely replanned path may be generated online.

The EPF-generated global path is combined with sonar sensor information in a two-layer FL inference engine. The first layer of the FL inference engine performs sensor fusion from sensor readings into the linguistic variable collision, providing information about potential *collisions* in four directions *front*, *back*, *left*, and *right*. The second layer guarantees collision avoidance with dynamic obstacles while following the trajectory generated by the potential field.

No assumptions are made on the amount of information contained in the environment *a priori* map (it may be completely empty) and on the shape of obstacles and their velocities. Environment map resolution depends on the "size" of the smallest possible grid cell. The EPF generated path complexity is linear with respect to the obstacle edges number within the environment [44]. Implementation on Nomadic Inc.'s *Cognos* software development system and the *Nomad 200* mobile robot platform [16] and experimental results demonstrate the effectiveness of the individual EPF, FL, and the combined EPF/FL approaches.

A comprehensive study of the problem and a survey of techniques used for navigational planning is given in [41], while a long list of additional references is given in [9] and [17]. Global planners may be classified into roadmaps (visibility graphs, Voronoi diagrams, freeway net, and silhouette) [21]–[27], cell decomposition approaches (exact and approximate) [28]–[31], and artificial potential field (APF) approaches [4], [6]–[10], [17]–[19], [33]. The actual electrostatic potential field [32], [36], [37] and the magnetic field [35] have been also used to solve specific navigation problems.